PUBLISHED VERSION

Michaela Waibel, Vanessa S. Solomon, Deborah A. Knight, Rachael A. Ralli, Sang-Kyu Kim, Kellie-Marie Banks, Eva Vidacs, Clemence Virely, Keith C.S. Sia, Lauryn S. Bracken, Racquel Collins-Underwood, Christina Drenberg, Laura B. Ramsey, Sara C. Meyer, Megu

Combined targeting of JAK2 and Bcl-2/Bcl-xL to cure mutant JAK2-driven malignancies and overcome acquired resistance to JAK2 inhibitors

Cell Reports, 2013; 5(4):1047-1059

Originally published at:
http://doi.org/10.1016/j.celrep.2013.10.038

Cell Reports
Article

Combined Targeting of JAK2 and Bcl-2/Bcl-xL to Cure Mutant JAK2-Driven Malignancies and Overcome Acquired Resistance to JAK2 Inhibitors

Michaela Waibel,[1,13] Vanessa S. Solomon,[1,13] Deborah A. Knight,[1] Rachael A. Ralli,[1] Sang-Kyu Kim,[1] Kellie-Marie Banks,[1] Eva Vidacs,[1] Clemence Virely,[2,3,4] Keith C.S. Sia,[5] Lauryn S. Bracken,[5] Racquel Collins-Underwood,[6] Christina Drenberg,[7] Laura B. Ramsey,[7] Sara C. Meyer,[8] Megumi Takiguchi,[9] Ross A. Dickins,[9] Ross Levine,[8] Jacques Ghysdael,[2,3,4] Mark A. Dawson,[10,11] Richard B. Lock,[5] Charles G. Mullighan,[6] and Ricky W. Johnstone[1,12,*]

[1]Cancer Therapeutics Program, The Peter MacCallum Cancer Centre, St. Andrews Place, East Melbourne, 3002 VIC, Australia
[2]Institut Curie, Centre Universitaire, Bat 110, 91405 Orsay, France
[3]Centre National de la Recherche Scientifique, Unite Mixte de Recherche 3306, Centre Universitaire, Bat 110, 91405 Orsay, France
[4]Institut National de la Sante et al Recherche Medicale, Unite 1005, Centre Universitaire, Bat 110, 91405 Orsay, France
[5]Children's Cancer Institute Australia for Medical Research, Lowy Cancer Research Centre, UNSW, Sydney, 2052 NSW, Australia
[6]Department of Pathology, St. Jude Children's Research Hospital, 262 Danny Thomas Place, Memphis, TN 38105, USA
[7]Department of Pharmaceutical Sciences, St. Jude Children's Research Hospital, 262 Danny Thomas Place, Memphis, TN 38105, USA
[8]Department of Medicine, Human Oncology and Pathogenesis Program and Leukemia Service, Memorial Sloan-Kettering Cancer Center, New York, NY 10065, USA
[9]Molecular Medicine Division, Walter and Eliza Hall Institute of Medical Research, Parkville, 3052 VIC, Australia
[10]Gurdon Institute and Department of Pathology, University of Cambridge, Tennis Court Road, Cambridge CB2 1QN, UK
[11]Department of Haematology, Cambridge Institute for Medical Research and Addenbrooke's Hospital, University of Cambridge, Hills Road, Cambridge CB2 0XY, UK
[12]Sir Peter MacCallum Department of Oncology, University of Melbourne, Parkville, 3052 VIC, Australia
[13]These authors contributed equally to this work
*Correspondence: ricky.johnstone@petermac.org
http://dx.doi.org/10.1016/j.celrep.2013.10.038

SUMMARY

To design rational therapies for JAK2-driven hematological malignancies, we functionally dissected the key survival pathways downstream of hyperactive JAK2. In tumors driven by mutant JAK2, Stat1, Stat3, Stat5, and the Pi3k and Mek/Erk pathways were constitutively active, and gene expression profiling of TEL-JAK2 T-ALL cells revealed the upregulation of prosurvival Bcl-2 family genes. Combining the Bcl-2/Bcl-xL inhibitor ABT-737 with JAK2 inhibitors mediated prolonged disease regressions and cures in mice bearing primary human and mouse JAK2 mutant tumors. Moreover, combined targeting of JAK2 and Bcl-2/Bcl-xL was able to circumvent and overcome acquired resistance to single-agent JAK2 inhibitor treatment. Thus, inhibiting the oncogenic JAK2 signaling network at two nodal points, at the initiating stage (JAK2) and the effector stage (Bcl-2/Bcl-xL), is highly effective and provides a clearly superior therapeutic benefit than targeting just one node. Therefore, we have defined a potentially curative treatment for hematological malignancies expressing constitutively active JAK2.

INTRODUCTION

The JAK tyrosine kinases (JAK1, JAK2, JAK3, and TYK2) are activated by cytokine receptor ligation leading to the subsequent phosphorylation and activation of STAT transcription factors (Ghoreschi et al., 2009). Activating JAK mutations have been identified in a range of human lymphoid and myeloid malignancies including pediatric and Down-syndrome-associated precursor-B-ALL (James et al., 2005; Mullighan et al., 2009b; Van Roosbroeck et al., 2011), and these JAK2 mutations are strong drivers of cellular transformation (Carron et al., 2000; Marty et al., 2010; Mullally et al., 2010). JAK2 fusion proteins, such as TEL-JAK2 detected in T- and B-ALL and BCR-ABL-negative chronic myeloid leukemia (CML), are another class of oncogenic gain-of-function JAK2 mutants (Van Roosbroeck et al., 2011). Mice expressing a TEL-JAK2 transgene under the control of the immunoglobulin heavy chain enhancer (EμTEL-JAK2) develop leukemia that is phenotypically similar to human T-ALL (Carron et al., 2000).

Small molecule JAK inhibitors (JAKi), such as the FDA-approved drug ruxolitinib (Pardanani, 2012), have been modestly successful in treating JAK2^{V617F}-driven myeloproliferative neoplasms (MPNs) (Atallah and Verstovsek, 2009; Santos and Verstovsek, 2011; Stein et al., 2011), whereas targeting JAK2 in ALL is still in experimental stages (Roberts et al., 2012; Sayyah and Sayeski, 2009), and responses of JAK2

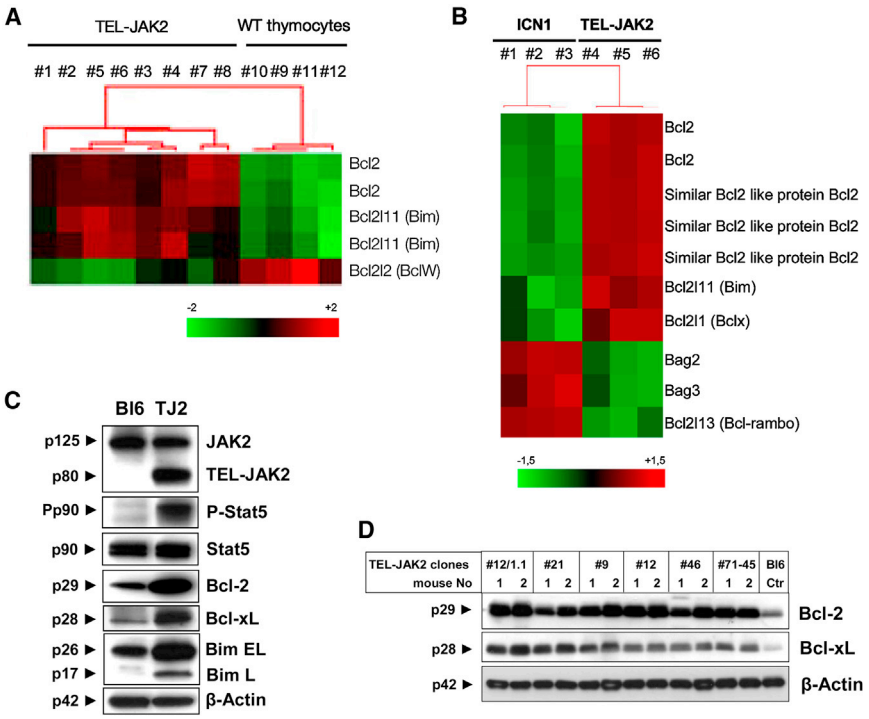

Figure 1. EμTEL-JAK2 Expression Is Associated with Elevated RNA and Protein Levels of Bcl-2, Bcl-x, and Bim

(A) Selected probe sets of transcript levels from thymocytes from four individual wild-type C57Bl/6 mice and eight EμTEL-JAK2 transgenic mice (>90% leukemic cells), analyzed using Affymetrix U74Av2 array. $p \leq 0.008$, false discovery rate 6.02%.

(B) Pangenomic Affymetrix 430 2.0 array was used to compare transcript levels in bone marrow cells from three independent ICN1 and TEL-JAK2 leukemic mice. Selected probe sets of differentially expressed Bcl-2 family members with a fold change of >0.5 or < -0.5 are shown. $p \leq 0.008$, false discovery rate 6.52%.

(C) Western blot analysis of C57Bl/6 thymocytes (Bl6) and EμTEL-JAK2 T-ALL cells (TJ2) to assess expression of JAK2, TEL-JAK2, P-Stat5, Stat5, Bcl-2, Bcl-xL, Bim, and the loading control β-actin.

(D) Western blot analysis of Bcl-2 and Bcl-xL in 6 independent TEL-JAK2 T-ALLs (two mice per tumor) compared to Bl6 thymocytes.

mutant ALL xenografts to ruxolitinib alone were variable (Maude et al., 2012). Furthermore, chronic exposure of mutant JAK2-expressing tumor cells to JAKi including ruxolitinib resulted in the outgrowth of drug-resistant cells with sustained JAK-STAT signaling through heterodimerization between activated JAK2 and JAK1 or TYK2 (Koppikar et al., 2012). A promising concept to reduce the evolution of tumors with acquired resistance to monotherapies and to improve therapeutic efficacy is by combining targeted therapies to concurrently inhibit two (or more) critical molecules within a single oncogenic network (Cragg et al., 2009; Knight et al., 2010; Maude et al., 2012).

With a view to designing effective therapeutic strategies for JAK2-driven hematological diseases, we examined the functional importance of various signaling pathways activated by oncogenic JAK2. We identified the key survival pathways downstream of active JAK2 and demonstrated that concurrent inhibition of aberrant JAK2 activity and the main effector molecules, Bcl-2 and Bcl-xL, induced prolonged disease regressions and cures in mice bearing established TEL-JAK2 T-ALL tumors. Furthermore, this combination was effective against xenotransplanted human JAK2 mutant precursor-B-ALL cells grown in immunocompromised mice. Moreover, our combination approach was effective against JAK2-driven tumor cells that had previously developed resistance to JAK2 inhibition. Given that BH3-mimetics and small molecule JAKi are in clinical development, our results argue for the initiation of clinical trials using a combination of these agents for the treatment of hematological malignancies driven by mutant JAK2.

RESULTS

Elevated Bcl-2 and Bcl-xL Levels in T-ALL Expressing the Constitutively Active TEL-JAK2 Fusion Protein

We previously developed the EμTEL-JAK2 mouse model of T-ALL (Carron et al., 2000), and comparative transcript profiling of TEL-JAK2 leukemia cells and normal C57BL/6 thymocytes revealed that expression of TEL-JAK2 was associated with a strong transcriptional upregulation of Bcl-2 and Bim (Figure 1A). Furthermore, comparative analysis with intracellular Notch-1 (ICN1)–driven T cell leukemia showed that increased expression of Bcl-2, Bcl-x, and Bim was specific for TEL-JAK2-expressing leukemic T cells (Figure 1B). TEL-JAK2 leukemias showed constitutive phosphorylation of Stat5 as previously observed (Carron et al., 2000; Lacronique et al., 1997) and elevated levels of Bcl-2, Bcl-xL, and Bim, compared to untransformed T cells (Figure 1C). Examination of independently arising EμTEL-JAK2 T-ALLs showed that all expressed relatively higher levels of Bcl-2 and Bcl-xL compared to untransformed C57BL/6 T cells (Figure 1D).

To determine if EμTEL-JAK2 T-ALLs were dependent on Bcl-2 or Bcl-xL for their survival in vitro, we treated the cells with varying concentrations of the BH3-mimetic, ABT-737 (Konopleva et al., 2006; Oltersdorf et al., 2005; Whitecross et al., 2009), or its less active enantiomer, ABT-737e. ABT-737 rapidly induced cell death in a dose- and caspase-dependent manner in different independently arising EμTEL-JAK2 T-ALLs (Figures 2A, S1A, and S1B). Consistent with the results shown in Figure 1B, EμTEL-JAK2 T-ALL cells were more sensitive to Bcl-2/Bcl-xL inhibition than ICN1-expressing T-ALL cells (Figure S1C), and

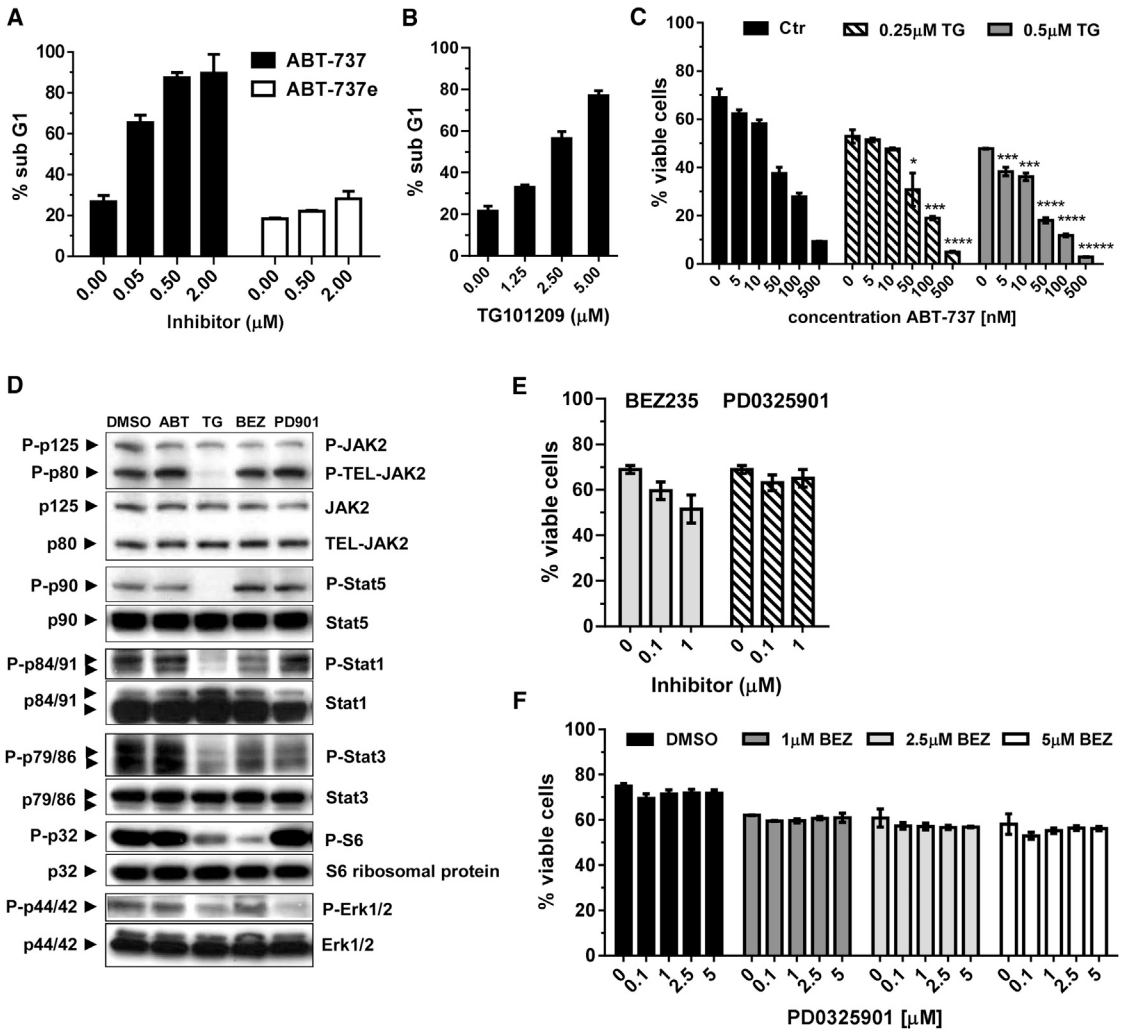

Figure 2. TEL-JAK2 T-ALL Cells Are Sensitive to the BH3 Mimetic ABT-737 and the JAK2 Inhibitor TG101209 and Show Constitutive Phosphorylation of Stat 1, Stat 3, Stat 5, and Mek/Erk and Pi3k/Akt Signaling

(A) TEL-JAK2 T-ALL cells were treated for 24 hr ex vivo with ABT-737 or enantiomer (ABT-737e), and cells with less than 2N DNA (% sub G1) were identified by flow cytometry.

(B) TEL-JAK2 T-ALL cells were treated for 24 hr ex vivo with increasing concentrations of TG101209. Cells with less than 2N DNA (% sub G1) were identified by flow cytometry.

(C) TEL-JAK2 T-ALL cells were treated for 24 hr ex vivo with increasing concentrations of ABT-737, ± 0.5 μM TG101209. Cell survival was measured by PI uptake (*for CI values, see Table S1).

(D) TEL-JAK2 T-ALL cells were treated with DMSO, ABT-737 (0.5 μM), TG101209 (1.5 μM), BEZ235 (1 μM), or PD0325901 (1 μM) for 1 hr, and western blot analysis was performed in order to detect phosphorylated and total Stat5, Stat1, Stat3, S6 ribosomal protein, and Erk1/2.

(E) TEL-JAK2 T-ALL cells were treated for 48 hr ex vivo with BEZ235 or PD0325901. Cell survival was measured by PI uptake.

(F) TEL-JAK2 T-ALL cells were treated for 24 hr ex vivo with PD0325901 (0.1–5 μM) ± BEZ235 (1–5 μM). Cell survival was measured by PI uptake.

Results in (A–C), (E), and (F) show mean ± SD of triplicates from one representative of at least three individual experiments. See also Figure S1.

B cell tumor cell lines expressing constitutively active mutant JAK2 were more sensitive to ABT-737 than cells expressing wild-type JAK2 (Figure S1D). Treatment of EμTEL-JAK2 T-ALL cells with the JAK2-selective inhibitor TG101209 (Pardanani et al., 2007) resulted in dose- and caspase-dependent apoptosis (Figures 2B and S1E). Selective killing of cells expressing mutant JAK2 by TG101209 was demonstrated by treating TEL-JAK2- and BCR-ABL1-expressing myeloid FDCP1 cells with TG101209, or a BCR-ABL1 kinase-specific inhibitor, Imatinib. FDCP1-TEL-JAK2 cells were highly sensitive to TG101209, but not to Imatinib, and, conversely, FDCP1-BCR-ABL1 cells were efficiently killed by Imatinib, whereas TG101209 treatment only had a minor effect with the highest concentrations used (Figure S1F).

We hypothesized that combining ABT-737 with TG101209 would be more potent than treatment with the single inhibitors. Treatment of EμTEL-JAK2 T-ALL cells with the combination resulted in enhanced killing of cells relative to either agent alone

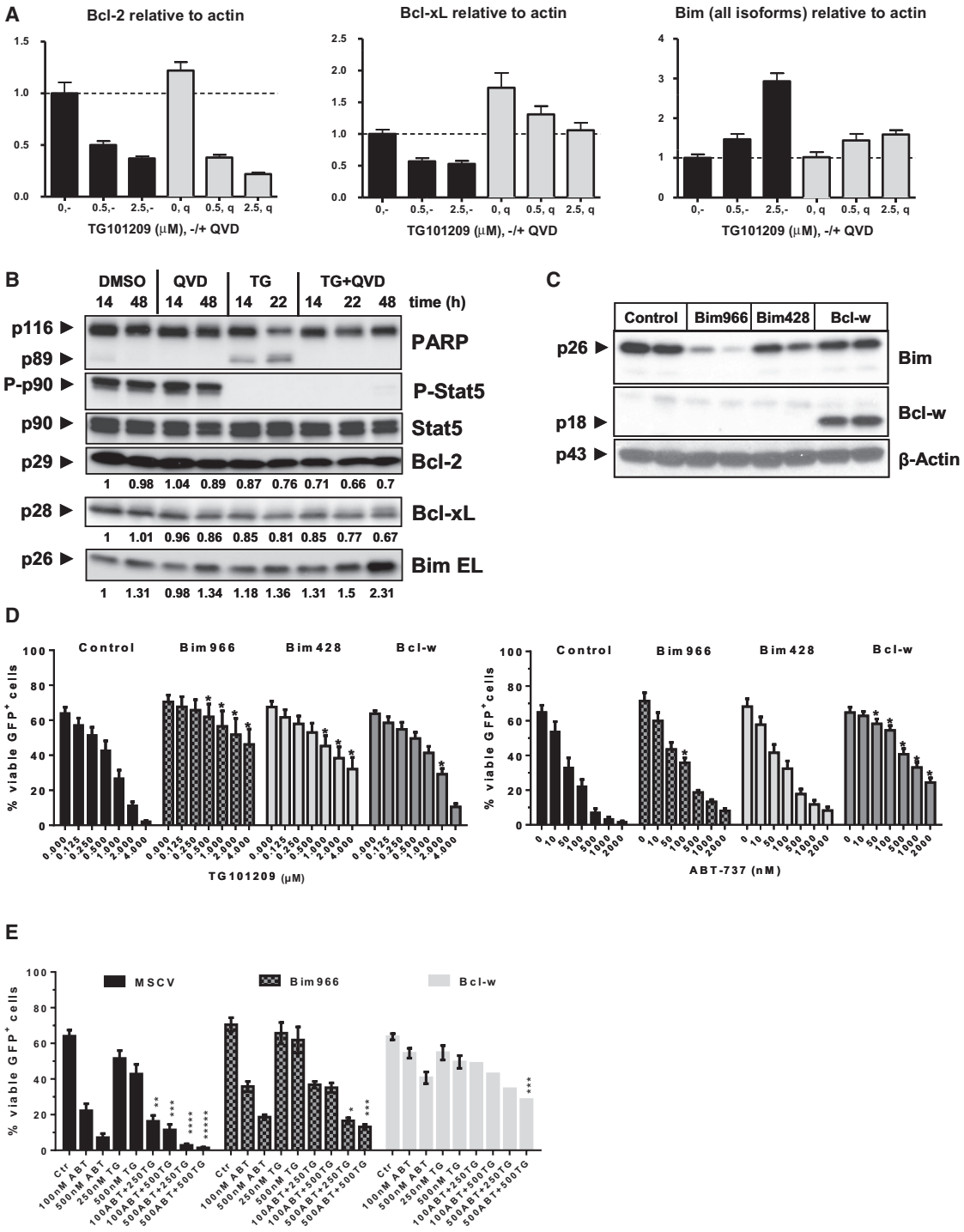

Figure 3. Inhibiting Constitutive JAK2 Activity Decreases mRNA and Protein Levels of Bcl-2 and Bcl-xL, while Increasing Bim Transcription and Protein Expression

(A) TEL-JAK2 T-ALL cells were treated with 0.5 or 2.5 μM TG101209 ± 50 μM QVD for 24 hr. mRNA levels for *bcl-2*, *bcl-xl*, and *bim* were determined by QPCR. Results shown are mean ± SD of triplicates from one representative of three independent experiments. See also Figure S2.

(B) TEL-JAK2 T-ALL cells were treated with DMSO, QVD (50 μM), TG101209 (2.5 μM), or TG101209 + QVD over 48 hr, and western blot analysis was performed to detect PARP, P-Stat5, Stat5, Bcl-2, Bcl-xL, and Bim. Expression levels relative to DMSO-treated controls are indicated by numbers beneath. Results shown are representative of three independent experiments.

(C) Western blot analysis of TEL-JAK2 T-ALL cells (two independent tumors per construct) expressing MSCV-IRES-GFP (Control), LMP-shBim.966 (shBim.966), LMP-shBim.428 (shBim.428), or MSCV-IRES-GFP-Bcl-w (Bcl-w) was performed to detect Bim, Bcl-w, and the loading control β-actin.

(legend continued on next page)

(Figure 2C; for confidence interval [CI] values, see Table S1). Similarly, this combined treatment resulted in a synergistic loss of cell viability in FDCP1-TEL-JAK2 cells, whereas FDCP1-BCR-ABL1 cells responded to a combination of Imatinib and ABT-737 (Figure S1G).

Identification of Signaling Pathways Important for Survival of TEL-JAK2 T-ALL Cells

To identify the key functional pathways downstream of activated JAK2, we assessed activation of Stat1, 3, and 5, Pi3k/Akt, and Mek/Erk in the presence and absence of TG101209. These pathways had been proposed to be important for the oncogenic effects of constitutively active JAK2 (Ho et al., 2002; Nguyen et al., 2001; Schwaller et al., 1998). TG101209 reduced the phosphorylation of TEL-JAK2, Stats 1, 3, and 5, S6 ribosomal protein, which is a marker of Pi3k pathway activity, and Erk1/2, which is a marker of Mek activation (Figure 2D). ABT-737 did not appreciably alter the expression or phosphorylation of any of these molecules. Treatment with the PI3K/mTOR inhibitor NVP-BEZ235 reduced phosphorylation of S6 and Stats 1 and 3, whereas the MEK inhibitor PD0325901 caused a reduction in Erk1/2 and Stat3 phosphorylation (Figure 2D). These data provide biochemical evidence that the Pi3k and Mek/Erk pathways are constitutively active in EμTEL-JAK2 T-ALL cells. However, NVP-BEZ235 caused only a slight loss of viability of EμTEL-JAK2 T-ALL cells at the on-target concentration of 1 μM (Figure 2E). Similarly, PD0325901 did not affect cell survival at concentrations that abrogated Erk1/2 phosphorylation (Figure 2E). Importantly, combining NVP-BEZ235 and PD0325901 did not result in a more substantial loss of cell viability than seen with the PI3K/mTOR inhibitor alone (Figure 2F).

Inhibition of TEL-JAK2 Regulates Bcl-2, Bcl-xL, and Bim Transcription and Protein Expression

TEL-JAK2 expression was associated with elevated levels of Bcl-2, Bcl-xL, and Bim, and recent studies indicated an important functional role for Bim in $JAK2^{V617F}$-expressing myeloid cell lines (Will et al., 2010). Treatment of EμTEL-JAK2 T-ALL cells with TG101209 reduced *bcl-2* and *bcl-xL* mRNA and protein levels but promoted the expression of *bim* (Figures 3A, 3B, and S2). To show the functional role of Bim in ABT-737- and TG101209-induced cell death, we knocked down Bim resulting in very good (shBim.966) and intermediate (shBim.428) depletion in EμTEL-JAK2 T-ALL tumors (Figure 3C). Bim knockdown modestly affected sensitivity to ABT-737, whereas TEL-JAK2-shBim cells showed significantly reduced sensitivity to TG101209 (Figure 3D) or the combination of ABT-737 and TG101209 (Figure 3E; for CI values, see Table S2).

Bcl-w levels were decreased in EμTEL-JAK2 T-ALL cells compared to wild-type T cells (Figure 1A), and we and others have shown that ABT-737 is a relatively weak inhibitor of Bcl-w (Mérino et al., 2012; Whitecross et al., 2009). Overexpression of Bcl-w (Figure 3C) led to significantly reduced sensitivity to ABT-737 (Figure 3D), had a minor effect on the responsiveness to TG101209 (Figure 3D), and substantially inhibited the combined effects of Bcl-2/Bcl-xL and JAK2 inhibition (Figure 3E; Table S2). Together, these results indicate that inhibition of JAK2 activity promotes the death of EμTEL-JAK2 T-ALL cells by reducing the levels of antiapoptotic proteins Bcl-2 and Bcl-xL, and promoting the accumulation of the potent proapoptotic protein, Bim.

Bcl-2/Bcl-xL and JAK2 Activity Is Critical for the Survival of EμTEL-JAK2 T-ALL Cells In Vivo

Mice bearing transplanted EμTEL-JAK2 T-ALL cells were treated with ABT-737, and within 8 hr this resulted in a substantial reduction in tumor cells in the peripheral blood concomitant with induction of tumor cell apoptosis and a significant reduction in spleen weight (Figures 4A, S3A, and S3C). These in vivo apoptotic effects of ABT-737 correlated with a significant increase in the survival of tumor-bearing mice (Figure 4B; *see Table S3 for statistical analysis). Similar results were observed using cohorts of mice transplanted with independently derived EμTEL-JAK2 T-ALL tumors (Figures S3B and S3D). Treatment of mice bearing EμTEL-JAK2 T-ALL tumors with ABT-737 and etoposide or cyclophosphamide resulted in significantly enhanced survival compared to mice treated with single agents (Figure 4C; *for p values, see Table S4). Importantly, a small number of tumor-bearing mice treated with chemotherapy plus ABT-737 showed complete therapeutic responses.

We next tested the response of EμTEL-JAK2 T-ALL cells in vivo to TG101209. Mice transplanted with EμTEL-JAK2 T-ALL cells demonstrated a substantial reduction in tumor cells in the peripheral blood and spleen after 4 days of treatment with TG101209 (Figure 4D). TG101209 also showed long-term therapeutic efficacy against EμTEL-JAK2 T-ALL cells in vivo, with treated mice demonstrating a significant increase in survival (median survival of 62 days) compared to the vehicle-treated group (median survival of 28 days, * $p = 0.0005$) (Figure 4E).

The Antileukemic Activity of JAK2 Inhibitors Is Greatly Enhanced by Concurrent Inhibition of Bcl-2/Bcl-xL

Next, the in vivo effects of combined abrogation of JAK2 activity by TG101209 and Bcl-2/Bcl-xL by ABT-737 were assessed. After adjusting the concentration of ABT-737 to achieve a well-tolerated combination dose, we treated tumor-bearing mice with TG101209 (100 mg/kg bid) and ABT-737 (25 mg/kg). This combination regimen rapidly and robustly reduced tumor cell counts in peripheral blood (Figure 5A). Importantly the combination of TG101209 and ABT-737 dramatically enhanced the survival of tumor-bearing mice with greater than 70% of treated

(D) TEL-JAK2 T-ALL cells expressing MSCV-IRES-GFP (Control), shBim.966, shBim.428, or Bcl-w were treated with TG101209 (0.125–4 μM) or ABT-737 (10–2,000 nM), and cell survival of GFP-expressing cells was measured by PI uptake. Results shown are mean ± SEM of three individual tumors each measured in duplicate (*$p < 0.05$ compared to TG101209 or ABT-737-treated control [MSCV vector] cells, respectively).

(E) TEL-JAK2-MSCV, -shBim.966, or -Bcl-w cells were treated with TG101209 (250 or 500 nM), ABT-737 (100 or 500 nM), or combinations of both, and cell survival of GFP-expressing cells was measured by PI uptake. Results show are mean ± SEM of three individual tumors each measured in duplicate; for combination treatment of Bcl-w-expressing cells, the mean of two individual tumors is shown (*for CI values, see Table S2).

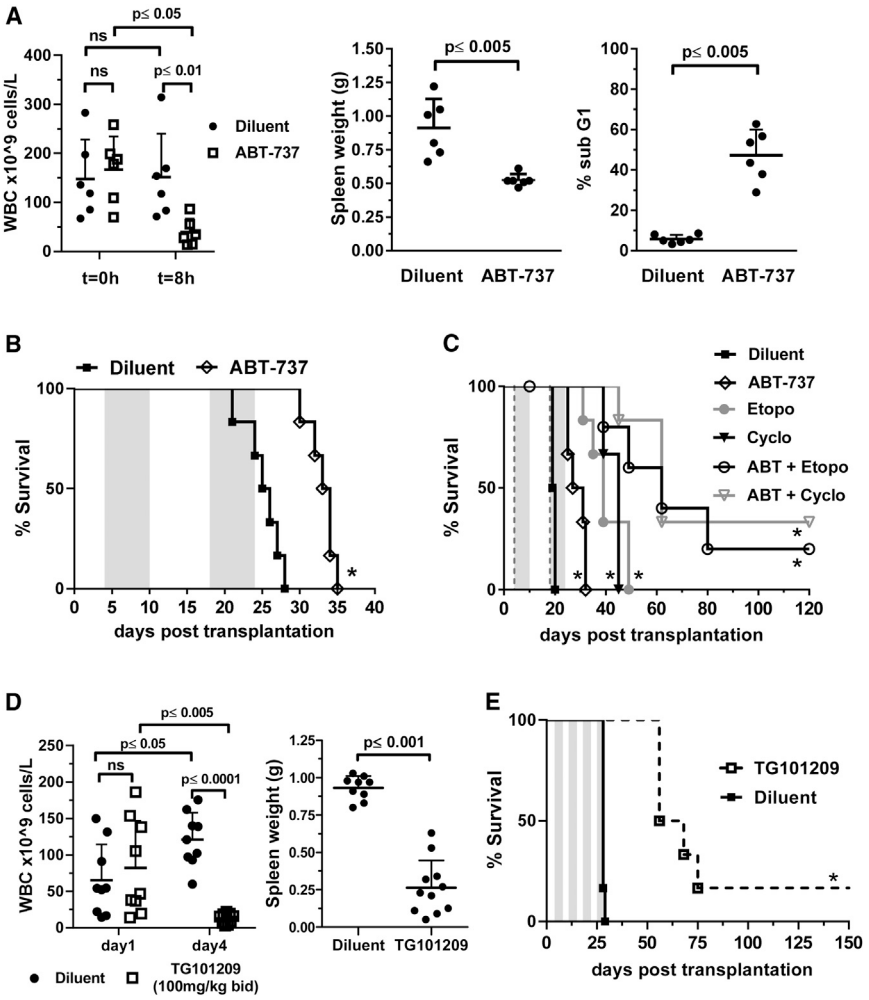

Figure 4. Therapeutic Effects of ABT-737 or of the JAK2 Inhibitor TG101209 in Mice Bearing EμTEL-JAK2 Leukemias

(A) Cohorts of mice (n = 6) bearing established EμTEL-JAK2 tumors were injected with a single dose of ABT-737 (75 mg/kg), sacrificed 8 hr after treatment, and analyzed for final white blood cell count (WBC), spleen weight, and induction of apoptosis (sub G1).

(B) Cohorts of mice (n = 6) transplanted with Eμ TEL-JAK2 cells were treated on day 4 posttransplant with ABT-737 (75 mg/kg) or diluent for 2 × 7 days separated by 7 days. Kaplan-Meier survival curves of mice treated with diluent (black line with squares) or ABT-737 (black dashed line with diamonds) are shown. See also Table S3 and Figure S3.

(C) Cohorts of mice (n = 6) transplanted with Eμ TEL-JAK2 cells were treated with two injections of etoposide (30 mg/kg) or cyclophosphamide (50 mg/kg) (days 4 and 18, dashed lines), alone or in combination with ABT-737 (75 mg/kg, 2 × 7 days). Kaplan-Meier survival curves of mice treated with diluent (black line with squares), ABT-737 (black line with open diamonds), etoposide (gray line with circles), cyclophosphamide (black line with triangles), ABT-737 + cyclophosphamide (gray line with open triangles), and ABT-737 + etoposide (black line with open circles) are shown. For statistical analysis, see Table S4.

(D) Cohorts of mice with secondary EμTEL-JAK2 ALL were treated with TG101209 (100 mg/kg bid PO) (n = 11) or vehicle control (n = 9) for 4 days. Peripheral blood was taken daily, and on day 4 mice were sacrificed and spleen weights were measured.

(E) Kaplan-Meier survival curves of cohorts of mice (n = 6) treated for 4 × 5 days with TG101209 (100 mg/kg bid PO) or vehicle control.

See also Figure S3.

mice remaining healthy more than 250 days after commencement of the dual therapy (Figure 5B; Table S5). Similar results were obtained using the structurally unrelated JAK2i NVP-BSK805 in combination with ABT-737 (Figure S4). These results clearly demonstrate that combined inhibition of oncogenic JAK2 and Bcl-2/Bcl-xL provides robust and sustained therapeutic responses in JAK2-driven malignancies resulting in mice cured of disease.

Combined Inhibition of JAK2 and Bcl-2/Bcl-xL Is Effective in Primary Human JAK2 Mutant B-ALL Cells

We next examined the effect of combined inhibition of JAK2 and Bcl-2/Bcl-xL in xenotransplanted human pre-B ALL cells expressing $JAK2^{R683G}$ or $JAK2^{T875N}$. Ex vivo, JAK2 mutant (Figures S5A and S5B) B-ALL cells were more sensitive to TG101209 alone, or TG101209 and ABT-737, compared to B-ALL cells with wild-type JAK2 ($JAK2^{wt}$) (Figure S5C). Furthermore, the combination of ABT-737 and TG101209 synergistically induced cell death in a panel of different JAK2 mutant pre-B-ALL xenografts cultured ex vivo (Figure S5D; Table S6), but not in various other primary ALL samples without known JAK2 mutations (Figure S5E). Similar to the results using Eμ TEL-JAK2 T-ALL cells (Figure 2D), treatment with the JAK2i TG101209 abrogated STAT5 phosphorylation and reduced levels of P-ERK in $JAK2^{R683G}$ and $JAK2^{T875N}$ pre-B-ALL samples, whereas P-STAT5 and P-ERK were not detectable in either untreated or treated $JAK2^{wt}$ cells (Figures S5A–S5C). Finally, we transplanted primary human pre-B-ALLs expressing $JAK2^{R683G}$ or $JAK2^{T875N}$ into NOD/Scid IL-2R$\gamma^{-/-}$ mice. Treatment of tumor-bearing mice with the combination of ABT-737 and TG101209 resulted in delayed tumor progression, and at the end of a 3 week treatment cycle tumor burden was significantly reduced with the combination compared to single-agent treatment (Figure 5C). Furthermore, only mice treated with TG101209 (100 mg/kg bid) and ABT-737 (25 mg/kg) showed a sustained therapeutic response (Figure 5D). This was also reflected in the survival of mice transplanted with $JAK2^{R867Q}$ B-ALL cells (also see Figure S5D for ex vivo dose response). TG101209 alone prolonged the survival of mice compared to control or ABT-737-treated mice, which was significantly enhanced by combining TG101209 and ABT-737 (Figure 5E; Table S7).

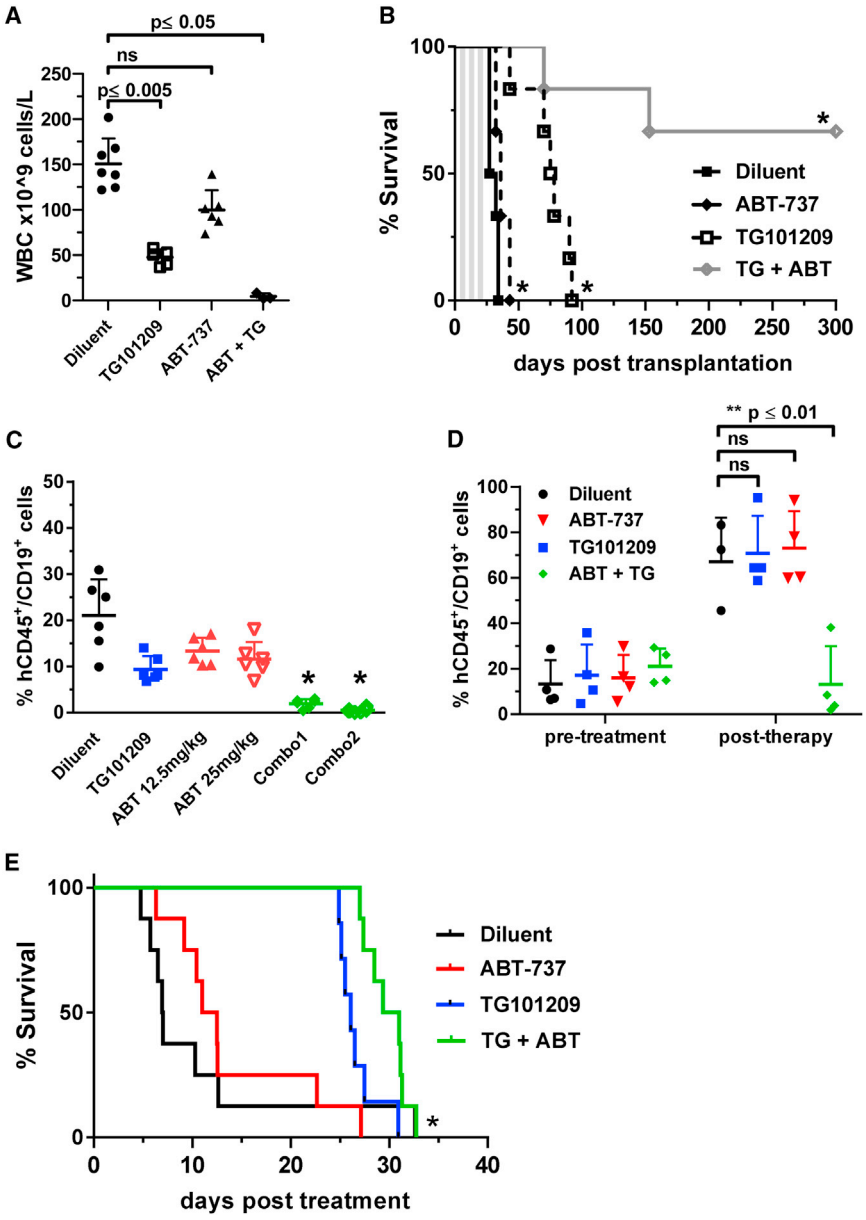

Figure 5. Therapeutic Effects of Combined Treatment with TG101209 and ABT-737 in Mice Bearing EμTEL-JAK2 Leukemias or Xenotransplanted with Human CRLF2 Rearranged/JAK2 Mutant Pre-B ALL

(A) Peripheral blood from cohorts of EμTEL-JAK2 leukemic mice treated with vehicle (n = 7), TG101209 (100 mg/kg bid PO) (n = 5), ABT-737 (25 mg/kg daily ip) (n = 6), or a combination of TG101209 and ABT-737 (n = 3) was taken and analyzed after 3 days of therapy.

(B) The survival curves of cohorts of mice (n = 6 per group) treated for 3 × 5 days separated by 2 days with the treatment regimen used under (A). See also Figure S4; *see Table S5 for statistical analysis.

(C) Cohorts of tumor bearing NOD/Scid IL-2Rγ$^{-/-}$ transplanted with primary human JAK2^{T875N} pre-B ALL cells were treated with diluent (n = 6), ABT-737 (12.5 and 25 mg/kg ip, n = 6), TG101209 (100 mg/kg bid PO, n = 6), or a combination of 12.5 mg/kg ABT-737 and TG101209 (combo 1) or 25 mg/kg ABT-737 and TG101209 (n = 6) (combo 2) for 3 × 5 days separated by 2 days. Peripheral blood was analyzed 2 days after therapy was ceased for hCD45 and hCD19 (*p < 0.005).

(D) Cohorts of NOD/Scid IL-2Rγ$^{-/-}$ transplanted with primary human JAK2^{R683G} pre-B ALL cells were treated with diluent (n = 5), ABT-737 (25 mg/kg ip, n = 4), TG101209 (100 mg/kg bid PO, n = 4), or a combination of both inhibitors (n = 4) for 3 × 5 days separated by 2 days. Peripheral blood was analyzed for hCD45- and hCD19-positive cells before and up to 2 weeks after therapy.

(E) The survival curves of cohorts of NOD/Scid IL-2Rγ$^{-/-}$ transplanted with primary human JAK2^{R687Q} pre-B ALL cells and treated as under (D) (n = 8 per group; * see Table S7 for statistical analysis).

See also Figure S4.

Dependence on Bcl-2/Bcl-xL Is a Feature of JAK2^{V617F}-Driven Malignancies

Oncogenic mutations in JAK2, particularly JAK2^{V617F}, are most prevalent in MPNs (Baxter et al., 2005; James et al., 2005; Kralovics et al., 2005; Levine et al., 2005). The human megakaryoblastic JAK2^{V617F} SET-2 cell line had constitutive phosphorylation of STATs1, 3, 5, ERK 1/2, and S6 that was abrogated by treatment with TG101209 (Figure 6A). Treatment with NVP-BEZ235 caused a substantial decrease in phospho-S6, a minor decrease in phospho-STAT3, and no change in phospho-ERK (Figure 6A). In contrast, PD0325901 strongly suppressed phospho-ERK but had little or no effect on the phosphorylation of other proteins analyzed (Figure 6A).

Treatment of SET-2 cells with TG101209 induced apoptosis in a dose-dependent manner (Figure 6B) concomitant with decreased levels of Bcl-2 and Bcl-xL, and an accumulation of Bim (Figures 6C and 6D). Furthermore, inhibiting JAK2 activity for 4 hr using TG101209 strongly decreased STAT5 bound to the *Bcl-xL* locus (Figure 6E), demonstrating a direct connection between JAK2 activity, STAT5 and transcriptional regulation of Bcl-xL. The viability of SET-2 cells was dependent on Bcl-2/Bcl-xL because treatment with ABT-737 induced a robust apoptotic response (Figure 6F). In contrast, treatment with on-target concentrations of NVP-BEZ235 or PD0325901 resulted in minimal death of SET-2 cells (Figure 6G), although ERK phosphorylation was completely blocked with the concentrations used here, and Bim levels were increased following MEK/ERK inhibition (data not shown). As with TEL-JAK2 T-ALL cells, combining TG101209 and ABT-737 was more effective in inducing apoptosis of SET-2 cells than either agent alone (Figure 6H; for CI values, see Table S8),

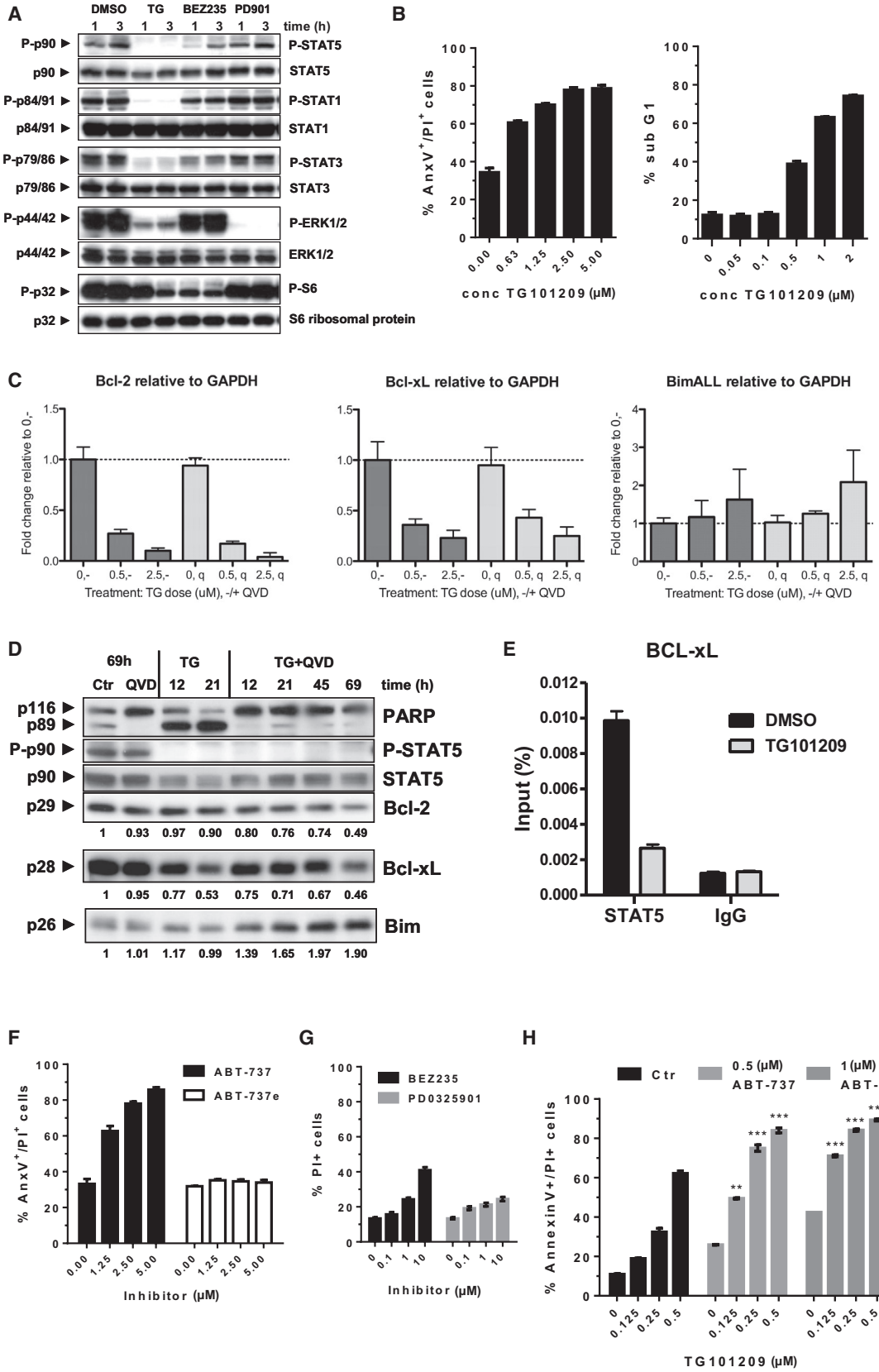

(legend on next page)

emphasizing the potential for combined inhibition of JAK2 and Bcl-2/Bcl-xL activity in the treatment of JAK2^{V617F}-expressing malignancies.

Acquired Resistance to JAK Inhibitors in JAK2^{V617F}-Driven MPN Cells Can Be Overcome by Combined Inhibition of JAK2 and Bcl-2/Bcl-xL

Chronic exposure of JAK2^{V617F} MPN cells to JAKi results in the outgrowth of drug-resistant cells, and we generated SET-2 cells with acquired resistance to TG101209 (SET-2-TGR) or ruxolitinib (SET-2-RuxR) as previously described (Koppikar et al., 2012) (Figure S6A). SET-2-TGR and SET-2-RuxR cells were clearly less sensitive to the both JAK2i compared to SET-2 cells grown for an equivalent period in vehicle alone (SET-2-Veh) (Figure 7A). SET-2 cells were effectively killed using relatively low concentrations of TG101209 and ABT-737 or ruxolitinib and ABT-737 for 48 hr (Figure S6B), and we were not able to obtain any proliferating cells from these cultures in the days following. SET-2-TGR and SET-2-RuxR cells were highly sensitive to combined treatment with TG101209 + ABT-737 or ruxolitinib + ABT-737 (Figure 7B). This effect was reproduced in a second, independently derived series of ruxolitinib-resistant SET-2 cells over a wide dose range of ruxolitinib + ABT-737 (Figure S6C). Taken together, these data indicate that combined inhibition of JAK2 and Bcl-2/Bcl-xL can overcome acquired resistance to single-agent JAK2i treatment.

SET-2-TGR and SET-2-RuxR cells demonstrated hyperphosphorylated JAK2, JAK1, TYK2, and STAT5 (Figure S6D), concomitant with elevated expression of Bcl-xL mRNA and protein (Figures 7C and 7D). Bim levels remained relatively unchanged, and remarkably the expression of Bcl-2 was decreased in SET-2-TGR and SET-2-RuxR cells compared to SET-2-Veh cells (Figures 7C and 7D). Based on these findings, we treated SET-2-TGR and SET-2-RuxR cells with ABT-737, the Bcl-2-specific inhibitor ABT-199 (Souers et al., 2013), or the Bcl-xL specific inhibitor WEHI-539 (Lessene et al., 2013) alone and in combination with TG101209 or ruxolitinib. Apoptosis of SET-2-TGR and SET-2-RuxR cells treated with TG101209 or ruxolitinib was strongly enhanced by ABT-737 and WEHI-539, but not ABT-199 (Figure 7E). The target selectivity of ABT-199 and WEHI-539 was demonstrated by treating Eμ-myc lymphomas overexpressing Bcl-2 or Bcl-xL with the BH3 mimetic drugs (Figures S6E and S6F).

The dynamic activation of the JAK2-STAT5-Bcl-xL axis through constant exposure to JAK2i was evident in SET-2-TGR and SET-2-RuxR cells 3 weeks after drug withdrawal (SET-2-TGRR and SET-2-RuxRR cells). Concomitant with the resensitization to JAK2i (Figure 7F), SET-2-TGRR and SET-2-RuxRR cells showed restoration of phospho-JAK2, -JAK1, -TYK2 and -STAT5, and Bcl-2 and Bcl-xL expression back to basal levels seen in SET-2-Veh cells (Figures S6G and S6H).

DISCUSSION

Chromosomal translocations or point mutations leading to expression of constitutively active JAK2 including TEL-JAK2 and JAK2^{V617F} have been identified in a range of human tumors (James et al., 2005; Mullighan et al., 2009b; Van Roosbroeck et al., 2011), and recently JAK2 point mutations (e.g., JAK2^{R683G}) and overexpression of the CRLF2 cytokine receptor have been identified as important factors in pre-B ALL (Harvey et al., 2010; Hertzberg et al., 2010; Mullighan et al., 2009a, 2009b). Ruxolitinib was the first JAKi approved by the FDA for the treatment of myelofibrosis (Pardanani, 2012), and others are currently in clinical trials for JAK2^{V617F}-driven MPNs (Santos and Verstovsek, 2011; Stein et al., 2011). Although JAKi therapy is able to reduce disease burden, it does not eradicate the disease-initiating malignant cell clone (Santos and Verstovsek, 2011; Stein et al., 2011), and single-agent ruxolitinib treatment in CRLF2 rearranged/JAK mutant xenograft models shows variable responses (Maude et al., 2012). Moreover, we have recently shown that continuous exposure of JAK2^{V617F+} SET-2 cells to JAKi results in acquired resistance through re-establishment of JAK-STAT signaling mediated by heterodimerization of JAK2 with JAK1 or TYK2 (Koppikar et al., 2012). This indicates that single-agent treatment with JAKi may only provide a transient therapeutic response and that additional treatment regimens designed to more effectively target hyperactivated JAK2 signaling may be required.

Our functional analysis of TEL-JAK2- and JAK2^{V617F}-expressing cells revealed constitutive activation of JAK-STAT, PI3K, and MEK/ERK signaling pathways consistent with other studies (Dai

Figure 6. SET-2^{V617F} Cells Show Constitutive Phosphorylation of STAT1, STAT3, STAT5, and MEK/ERK and PI3K Signaling and Are Sensitive to TG101209 and ABT-737

(A) SET-2^{V617F} cells were treated with DMSO, TG101209 (1 μM), BEZ235 (5 μM), or PD0325901 (5 μM) for 1 or 3 hr, and lysates were used for western blot analysis of phosphorylated STAT5, STAT1, STAT3, S6 ribosomal protein, and ERK1/2.

(B) Induction of cell death in SET-2^{V617F} cells treated with increasing concentrations of TG101209 (AnxV/PI staining 24 hr posttreatment, DNA fragmentation after 48 hr).

(C) SET-2^{V617F} cells were treated with 0.5 or 2.5 μM TG101209 ± 50 μM QVD for 24 hr, and mRNA levels for *bcl-2*, *bcl-xL*, and *bim* were determined by QPCR. Results shown are mean ± SD of triplicates from one representative of three individual experiments.

(D) SET-2^{V617F} cells were treated with DMSO (69 hr), QVD (20 μM, 69 hr), TG101209 (2.5 μM), or TG101209 + QVD for up to 69 hr and subjected to western blot analysis to detect PARP, P-, and total STAT5, Bcl-2, Bcl-xL, and Bim. Expression levels relative to DMSO-treated controls are indicated by numbers beneath. Results shown are representative of two independent experiments.

(E) SET-2^{V617F} cells were treated for 4 hr with 1 μM TG101209 or DMSO (vehicle). Chromatin from these cells was used in ChIP assays followed by QPCR. Data from biological replicate experiments are represented as the bound over input percentage. Results shown are mean ± SD of replicate experiments.

(F and G) (F) SET-2^{V617F} cells treated with ABT-737 or Enantiomer (ABT-737e) were analyzed for 2N DNA content (% sub G1) and (G) cell death 48 hr posttreatment with BEZ235 (0.1–10 μM) or PD0325901 (0.1–10 μM) determined by PI exclusion.

(H) Cell death induced by cotreatment of SET-2^{V617F} cells with increasing concentrations of TG101209 ± 0.5 or 1 μM ABT-737 after 48 hr was determined by AnxV/PI staining. (***synergism/**moderate synergism; for CI values, see Table S8).

Results shown in (F)–(H) are mean ± SD from triplicates of one representative of three individual experiments. See also Figure S5.

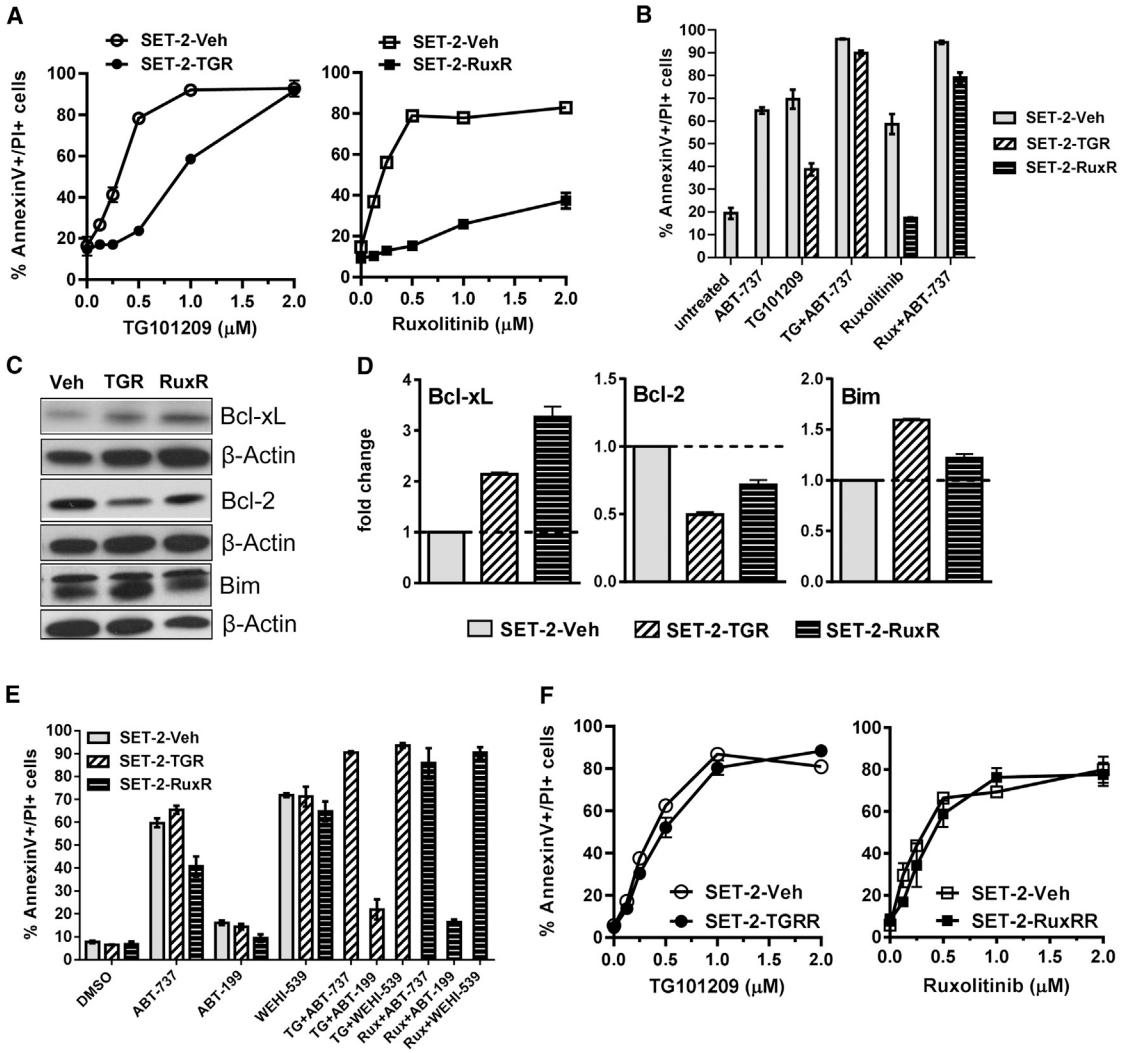

Figure 7. JAK Inhibitor Resistance in SET-2^{V617F} Cells Can Be Overcome by Combinations of ABT-737 and TG101209 or Ruxolitinib and Is Predominantly Bcl-xL Dependent

(A) DMSO-treated control cells (SET-2-Veh) and TG101209- or ruxolitinib-resistant SET-2 cells (SET-2-TGR, -RuxR) were treated with increasing concentrations of TG101209 (0.125–2 μM) or ruxolitinib (0.125–2 μM), and cell death was measured by AnnexinV/PI staining after 48 hr. Graphs shown are mean ± SD from triplicates of one of three independent experiments.

(B) Vehicle controls and TG101209- and ruxolitinib-resistant SET-2 cells were treated with either 1.6 μM ABT-737, 0.6 μM TG101209, 0.3 μM ruxolitinib, ABT-737 + TG101209, or ABT-737 + ruxolitinib, and cell death was measured after 48 hr by staining with AnnexinV/PI. Graphs shown are mean ± SD of triplicates from one of three individual experiments.

(C) Lysates from SET-2-Veh, -TGR, and -RuxR cells were used for western blot analysis of Bcl-2, Bcl-xL, and Bim. β-actin was used as a loading control.

(D) mRNA levels of *bcl-2*, *bcl-xL*, and *bim* in SET-2-Veh, -TGR, or -RuxR were determined by QPCR. Results shown are mean ± SD of triplicates from one representative of two individual experiments.

(E) Vehicle controls and TG101209 and ruxolitinib-resistant SET-2 cells were treated with 1.6 μM ABT-737 or ABT-199, 0.8 μM WEHI-539, 0.6 μM TG101209, or 0.3 μM ruxolitinib or combinations of ABT-737, ABT-199, or WEHI-539 with TG101209 or ruxolitinib, and cell death was measured after 48 hr by AnnexinV/PI staining. Graphs shown are mean ± SD of triplicates from one of two individual experiments.

(F) Vehicle-treated and resensitized SET-2 cells (3 weeks after JAKi withdrawal) were treated with increasing concentrations of TG101209 (0.125–2 μM) or ruxolitinib (0.125–2 μM), and cell death was measured by AnnexinV/PI staining after 48 hr. Graphs shown are mean ± SD from triplicates of one of two independent experiments.

See also Figure S6.

et al., 2005; Ho et al., 2002; Röder et al., 2001). Using TG101209, we demonstrated the addiction of JAK2 mutant cells to activated JAK2 for survival both in vitro and in vivo; however, inhibiting PI3K/mTOR or MEK activity alone or in combination did not substantially affect tumor cell viability. This indicates that although multiple oncogenic pathways are regulated by JAK2 activity, not all are essential for malignant cell survival. We demonstrated JAK2-driven expression of Bcl-2 and Bcl-xL in EμTEL-JAK2

T-ALL and SET-2 cells consistent with elevated levels of these prosurvival proteins in samples from patients with JAK2^{V617F}-driven MPNs (Silva et al., 1998; Zeuner et al., 2009). JAK2 mutant cells were sensitive to ABT-737, and this effect was suppressed by overexpression of Bcl-w, in accordance with studies by us and others showing that ABT-737 is a relatively weak inhibitor of Bcl-w (Mérino et al., 2012; Whitecross et al., 2009). Bim levels were elevated in EμTEL-JAK2 T-ALL and SET-2 cells treated with JAK2i and consistent with the proposed functional role of Bim in mediating cell death following JAK2^{V617F} inhibition (Will et al., 2010); depletion of Bim in EμTEL-JAK2 T-ALL cells reduced their sensitivity to TG101209. Although treatment with a MEK/ERK inhibitor also led to increased Bim protein levels, neither MEK/ERK nor PI3K inhibition alone or in combination induced substantial death of cells expressing mutant JAK2. Thus, upregulation of Bim was necessary, yet not sufficient to induce death of tumors expressing mutant JAK2. We posit that Bcl-2 and Bcl-xL are important downstream targets of oncogenic JAK2 and speculate that the ratio of Bcl-2/Bcl-xL and Bim is decisive for cell survival or death in tumors addicted to mutant JAK2.

By using a JAK2i, which decreases Bcl-2/Bcl-xL and increases Bim levels, and adding ABT-737, the canonical JAK/STAT–Bcl-2/Bcl-xL axis was specifically targeted at two levels resulting in remarkable therapeutic effects in vivo and minimal toxicity. Other recently suggested therapeutic approaches include combining JAKi with inhibitors of HSP90 or the PI3K/mTOR inhibitor BEZ235 (Fiskus et al., 2013; Weigert et al., 2012). These combinations achieved promising results in vitro, and in our hands TG101209 in combination with either BEZ235 or the HSP90 inhibitors 17-AAG and Radicicol induced a moderate and mostly additive loss of cell viability (data not shown). HSP90 inhibition destabilizes various HSP90-client proteins, including JAK2 (Weigert et al., 2012; data not shown), therefore potentially negatively regulating JAK-STAT signaling. However, treatment of mice xenotransplanted with human CRLF2 rearranged pre-B ALL-expressing mutant or wild-type JAK2 with a JAK2i in combination with the HSP90 inhibitor AUY922 did not lead to an improved survival of these mice compared to the single inhibitor groups (Weigert et al., 2012). Moreover, combining BEZ235 with TG101209 was not able to enhance BEZ235-induced cell death in TG101209-resistant MPN cells (Fiskus et al., 2013), indicating that this combination would be less effective than the ABT-737/JAK2i treatment. This furthermore emphasizes the potential of coordinated inhibition of JAK2 and prosurvival Bcl-2 proteins in JAK2-driven MPN and ALL.

An important finding from our study was that the combination of JAK2i and ABT-737 prevented the outgrowth of JAK2^{V617F}-expressing MPN cells with acquired resistance to single agents. Moreover, as we have recently described (Koppikar et al., 2012), cells chronically treated with JAK2i reversibly hyperactivated the JAK2/STAT5 signaling axis. Our data extend these studies showing that this resulted in increased expression of Bcl-xL and surprisingly decreased levels of Bcl-2. We demonstrated that SET-2-TGR and SET-2-RuxR remained sensitive to combination treatment with JAK2i and ABT-737 or the Bcl-xL specific inhibitor WEHI-539; however, the Bcl-2-specific inhibitor ABT-199 was ineffective in combination with JAK2 inhibition. We therefore posit that the JAK2/STAT5/Bcl-xL axis is an important survival pathway for JAK2^{V617F}-driven MPN cells and that combined targeting of the JAK2 oncogenic signaling pathway at two critical nodes—one being JAK2 activity itself, the other being Bcl-xL—is clearly superior to treatment with single inhibitors alone. Our data provide evidence that this combined approach will have strong efficacy in the treatment of ALL driven by mutated JAK2 and the potential to circumvent and overcome acquired resistance to single-agent JAK inhibitor therapy.

EXPERIMENTAL PROCEDURES

Microarray

Gene expression analysis was performed using the Murine Genome U74Av2 GeneChip (TEL-JAK2 versus wild-type thymocytes), and the Murine Genome 430 2.0 GeneChip (TEL-JAK2 versus ICN1 bone marrow cells, >50% leukemic cells in all samples) (Affymetrix). Total RNA was isolated using the RNeasy kit (Qiagen) and cRNA synthesis, labeling, hybridization, washing, and scanning were performed according to the manufacturer's protocol (Affymetrix). Student's t test was used to select significant genes ($p \leq 0.008$), and Cluster and Treeview software were used to cluster tumor samples according to their Bcl-2 gene expression pattern as assessed by hierarchical clustering using the complete linkage mode.

In Vivo Assays

All animal work was conducted under the current "Australian Code of Practice for the Care and Use of Animals for Scientific Purposes" and approved by the Peter MacCallum Animal Experimental Ethics Committee. TEL-JAK2 T-ALL cells from spleen, lymph node, or thymus of C57Bl/6:Eμ-TEL-JAK2 transgenic mice were transplanted by intravenous injection into 6- to 8-week-old C57Bl/6:Ly5.2 and C75Bl/6:Ly5.1 mice. Blood was taken by retroorbital or tail bleed, and white blood cell counts were analyzed using the Advia 120 Hematology System (Siemens Healthcare Diagnostics). Xenotransplantation experiments were performed by intravenous injection of human pre-B ALL cells into 6- to 10-week-old NOD/Scid IL-2R$\gamma^{-/-}$ mice. Engraftment was monitored by staining blood samples with antihuman CD45-APC-H7 and CD19-PE-Cy7 antibodies (BD Biosciences). Therapy was commenced when tumor burden in peripheral blood was $\geq$5%. For detailed description of drug administration, statistical analysis, and retroviral transduction of TEL-JAK2 tumor cells, see the Supplemental Experimental Procedures.

Cell Viability Assays

Detailed descriptions of cell growth conditions are included in the supplemental experimental procedures. Cells were either stained in PBS + 1 μg/ml propidium iodide (PI) (Sigma-Aldrich) or in 10 mM HEPES/NaOH [pH 7.4], 140 mM NaCl, 5 mM $CaCl_2x2H_2O$ using 1 μg/ml propidium iodide and fluorescein-isothiocyanate- or APC-conjugated AnnexinV (BD Biosciences) used 1:100. DNA fragmentation was measured by staining cells in hypotonic 0.1% Na-citrate/0.1% Triton X-100 buffer with 50 μg/ml PI. Cell-surface staining of human pre-B ALL cells was performed using antihuman CD45-APC-H7 and CD19-PE-Cy7 antibodies (BD Biosciences). All experiments were analyzed on a BD FACS Canto II using the FlowJo analysis software (Tree Star).

Western Blot

Western blot analysis of whole-cell lysates was performed as previously described (Whitecross et al., 2009) using primary antibodies against phospho-JAK2 Tyr1007/1008, JAK2 (D2E12), P-STAT5 Tyr694, STAT5 (3H7), P-STAT3 Tyr705, STAT3, P-STAT1 Tyr701, P-S6 Ser240/244, S6 ribosomal protein, P-ERK Thr202/Tyr204, ERK, PARP (46D11) (Cell Signaling Technology), STAT1, Bcl-xL, mouse Bcl-2 (BD Biosciences), human Bcl-2 (Santa Cruz Biotechnology), Bim/BOD (Enzo Life Sciences), and β-actin (Sigma-Aldrich).

RNA Isolation and Quantitative Real-Time PCR

RNA was isolated using the QIAGEN RNeasy Midi Kit, following the manufacturers' instructions. Quality and final concentration of RNA was determined using a Nanodrop (Thermo Scientific) and cDNA prepared using MMLV reverse transcriptase and random primers (Promega). Quantitative real-time PCR (qPCR) was performed by using 150 nM each of forward and reverse primers, SYBR Green Master Mix including ROX size standard (Applied Biosystems). Reaction mixtures were prepared in triplicate for each cDNA sample and incubated in an Applied Biosystems 7900HT Real-Time instrument according to the following program: 95°C, 10 min; 40 cycles of 95°C for 30 s, 60°C for 30 s; 95°C for 15 s; 60°C for 15 s; 95°C for 15 s, with a ramp rate of 2% from 60°C to 95°C. Expression levels for human genes were normalized by comparison with expression of GAPDH, whereas murine genes were normalized by comparison with expression of β-actin. For primer sequences, see the Supplemental Experimental Procedures.

Chromatin Immunoprecipitation Assay

Chromatin immunoprecipitation (ChIP) was performed as previously described (Dawson et al., 2009). Immunoprecipitated DNA was analyzed on an ABI 7900 real-time PCR machine, using TaqMan PCR mastermix according to the manufacturer's instructions. The following primers and probes were used in the analysis. Primer sequences used for human Bcl-xL were forward 5′-TGGTATCCTCACAACAAACTtcatg-3′; reverse 5′-gaggctggcagctgaattg-3′; TaqMan probe 5′-[Fam]ttatcttcctccaactctgacctgt[Tam]-3′.

ACCESSION NUMBERS

Microarray data were deposited in the NCBI Gene Expression Omnibus database and are available under accession number GSE51250.

SUPPLEMENTAL INFORMATION

Supplemental Information includes Supplemental Experimental Procedures, six figures, and eight tables and can be found with this article online at http://dx.doi.org/10.1016/j.celrep.2013.10.038.

ACKNOWLEDGMENTS

R.W.J. is a Principal Research Fellow of the National Health and Medical Research Council of Australia (NHMRC) and is supported by NHMRC Program and Project Grants, Susan G. Komen Breast Cancer Foundation, Prostate Cancer Foundation of Australia, Cancer Council Victoria, Leukemia Foundation of Australia, Victorian Breast Cancer Research Consortium, Victorian Cancer Agency, and Australian Rotary Health Foundation. M.W. was supported by a fellowship from the Deutsche Forschungsgemeinschaft and funding from the NHMRC. V.S.S. received funding from the NHMRC, the Peter MacCallum Cancer Foundation, and Bioplatforms Australia. S.C.M. received funding from the Swiss National Science Foundation and the Huggenberger-Bischoff Foundation for Cancer Research. R.A.D. is a Sylvia and Charles Viertel Foundation Senior Medical Research Fellow. R.B.L. is a Senior Research Fellow of the NHMRC. C.G.M. is supported by ALSAC of St. Jude Children's Research Hospital and the Pew Charitable Trusts. Work in J.G.'s laboratory was supported by funds from Institute Curie, CNRS, INSERM, INCA, and Ligue Contre le Cancer (Equipe labellisee Ligue). M.A.D. is a Wellcome-Beit Intermediate Clinical Fellow. We thank Drs. J. Shortt, M. Bishton, E. Hawkins, K. Hannan, K. Kinross, A. Alsop, and D. Ritchie for valuable discussions and reagents, K. Stanley for technical assistance, and the Tissue Resources Laboratory of St. Jude Children's Research Hospital for patient samples. We thank Novartis, Sanofi-Aventis, and Abbott for supply of reagents. Children's Cancer Institute Australia for Medical Research is affiliated with the University of New South Wales and the Sydney Children's Hospitals Network. JAK2 mutant xenografts were established in collaboration with the Children's Oncology Group.

Received: September 28, 2012
Revised: July 17, 2013
Accepted: October 22, 2013
Published: November 21, 2013

REFERENCES

Atallah, E., and Verstovsek, S. (2009). Prospect of JAK2 inhibitor therapy in myeloproliferative neoplasms. Expert Rev. Anticancer Ther. *9*, 663–670.

Baxter, E.J., Scott, L.M., Campbell, P.J., East, C., Fourouclas, N., Swanton, S., Vassiliou, G.S., Bench, A.J., Boyd, E.M., Curtin, N., et al.; Cancer Genome Project. (2005). Acquired mutation of the tyrosine kinase JAK2 in human myeloproliferative disorders. Lancet *365*, 1054–1061.

Carron, C., Cormier, F., Janin, A., Lacronique, V., Giovannini, M., Daniel, M.T., Bernard, O., and Ghysdael, J. (2000). TEL-JAK2 transgenic mice develop T-cell leukemia. Blood *95*, 3891–3899.

Cragg, M.S., Harris, C., Strasser, A., and Scott, C.L. (2009). Unleashing the power of inhibitors of oncogenic kinases through BH3 mimetics. Nat. Rev. Cancer *9*, 321–326.

Dai, C., Chung, I.J., and Krantz, S.B. (2005). Increased erythropoiesis in polycythemia vera is associated with increased erythroid progenitor proliferation and increased phosphorylation of Akt/PKB. Exp. Hematol. *33*, 152–158.

Dawson, M.A., Bannister, A.J., Göttgens, B., Foster, S.D., Bartke, T., Green, A.R., and Kouzarides, T. (2009). JAK2 phosphorylates histone H3Y41 and excludes HP1alpha from chromatin. Nature *461*, 819–822.

Fiskus, W., Verstovsek, S., Manshouri, T., Smith, J.E., Peth, K., Abhyankar, S., McGuirk, J., and Bhalla, K.N. (2013). Dual PI3K/AKT/mTOR inhibitor BEZ235 synergistically enhances the activity of JAK2 inhibitor against cultured and primary human myeloproliferative neoplasm cells. Mol. Cancer Ther. *12*, 577–588.

Ghoreschi, K., Laurence, A., and O'Shea, J.J. (2009). Janus kinases in immune cell signaling. Immunol. Rev. *228*, 273–287.

Harvey, R.C., Mullighan, C.G., Chen, I.M., Wharton, W., Mikhail, F.M., Carroll, A.J., Kang, H., Liu, W., Dobbin, K.K., Smith, M.A., et al. (2010). Rearrangement of CRLF2 is associated with mutation of JAK kinases, alteration of IKZF1, Hispanic/Latino ethnicity, and a poor outcome in pediatric B-progenitor acute lymphoblastic leukemia. Blood *115*, 5312–5321.

Hertzberg, L., Vendramini, E., Ganmore, I., Cazzaniga, G., Schmitz, M., Chalker, J., Shiloh, R., Iacobucci, I., Shochat, C., Zeligson, S., et al. (2010). Down syndrome acute lymphoblastic leukemia, a highly heterogeneous disease in which aberrant expression of CRLF2 is associated with mutated JAK2: a report from the International BFM Study Group. Blood *115*, 1006–1017.

Ho, J.M., Nguyen, M.H., Dierov, J.K., Badger, K.M., Beattie, B.K., Tartaro, P., Haq, R., Zanke, B.W., Carroll, M.P., and Barber, D.L. (2002). TEL-JAK2 constitutively activates the extracellular signal-regulated kinase (ERK), stress-activated protein/Jun kinase (SAPK/JNK), and p38 signaling pathways. Blood *100*, 1438–1448.

James, C., Ugo, V., Le Couédic, J.P., Staerk, J., Delhommeau, F., Lacout, C., Garçon, L., Raslova, H., Berger, R., Bennaceur-Griscelli, A., et al. (2005). A unique clonal JAK2 mutation leading to constitutive signalling causes polycythaemia vera. Nature *434*, 1144–1148.

Knight, Z.A., Lin, H., and Shokat, K.M. (2010). Targeting the cancer kinome through polypharmacology. Nat. Rev. Cancer *10*, 130–137.

Konopleva, M., Contractor, R., Tsao, T., Samudio, I., Ruvolo, P.P., Kitada, S., Deng, X., Zhai, D., Shi, Y.X., Sneed, T., et al. (2006). Mechanisms of apoptosis sensitivity and resistance to the BH3 mimetic ABT-737 in acute myeloid leukemia. Cancer Cell *10*, 375–388.

Koppikar, P., Bhagwat, N., Kilpivaara, O., Manshouri, T., Adli, M., Hricik, T., Liu, F., Saunders, L.M., Mullally, A., Abdel-Wahab, O., et al. (2012). Heterodimeric JAK-STAT activation as a mechanism of persistence to JAK2 inhibitor therapy. Nature *489*, 155–159.

Kralovics, R., Passamonti, F., Buser, A.S., Teo, S.S., Tiedt, R., Passweg, J.R., Tichelli, A., Cazzola, M., and Skoda, R.C. (2005). A gain-of-function mutation of JAK2 in myeloproliferative disorders. N. Engl. J. Med. *352*, 1779–1790.

Lacronique, V., Boureux, A., Valle, V.D., Poirel, H., Quang, C.T., Mauchauffé, M., Berthou, C., Lessard, M., Berger, R., Ghysdael, J., and Bernard, O.A. (1997). A TEL-JAK2 fusion protein with constitutive kinase activity in human leukemia. Science *278*, 1309–1312.

Lessene, G., Czabotar, P.E., Sleebs, B.E., Zobel, K., Lowes, K.N., Adams, J.M., Baell, J.B., Colman, P.M., Deshayes, K., Fairbrother, W.J., et al. (2013). Structure-guided design of a selective BCL-X(L) inhibitor. Nat. Chem. Biol. *9*, 390–397.

Levine, R.L., Wadleigh, M., Cools, J., Ebert, B.L., Wernig, G., Huntly, B.J., Boggon, T.J., Wlodarska, I., Clark, J.J., Moore, S., et al. (2005). Activating mutation in the tyrosine kinase JAK2 in polycythemia vera, essential thrombocythemia, and myeloid metaplasia with myelofibrosis. Cancer Cell *7*, 387–397.

Marty, C., Lacout, C., Martin, A., Hasan, S., Jacquot, S., Birling, M.C., Vainchenker, W., and Villeval, J.L. (2010). Myeloproliferative neoplasm induced by constitutive expression of JAK2V617F in knock-in mice. Blood *116*, 783–787.

Maude, S.L., Tasian, S.K., Vincent, T., Hall, J.W., Sheen, C., Roberts, K.G., Seif, A.E., Barrett, D.M., Chen, I.M., Collins, J.R., et al. (2012). Targeting JAK1/2 and mTOR in murine xenograft models of Ph-like acute lymphoblastic leukemia. Blood *120*, 3510–3518.

Mérino, D., Khaw, S.L., Glaser, S.P., Anderson, D.J., Belmont, L.D., Wong, C., Yue, P., Robati, M., Phipson, B., Fairlie, W.D., et al. (2012). Bcl-2, Bcl-x(L), and Bcl-w are not equivalent targets of ABT-737 and navitoclax (ABT-263) in lymphoid and leukemic cells. Blood *119*, 5807–5816.

Mullally, A., Lane, S.W., Ball, B., Megerdichian, C., Okabe, R., Al-Shahrour, F., Paktinat, M., Haydu, J.E., Housman, E., Lord, A.M., et al. (2010). Physiological Jak2V617F expression causes a lethal myeloproliferative neoplasm with differential effects on hematopoietic stem and progenitor cells. Cancer Cell *17*, 584–596.

Mullighan, C.G., Collins-Underwood, J.R., Phillips, L.A., Loudin, M.G., Liu, W., Zhang, J., Ma, J., Coustan-Smith, E., Harvey, R.C., Willman, C.L., et al. (2009a). Rearrangement of CRLF2 in B-progenitor- and Down syndrome-associated acute lymphoblastic leukemia. Nat. Genet. *41*, 1243–1246.

Mullighan, C.G., Zhang, J., Harvey, R.C., Collins-Underwood, J.R., Schulman, B.A., Phillips, L.A., Tasian, S.K., Loh, M.L., Su, X., Liu, W., et al. (2009b). JAK mutations in high-risk childhood acute lymphoblastic leukemia. Proc. Natl. Acad. Sci. USA *106*, 9414–9418.

Nguyen, M.H., Ho, J.M., Beattie, B.K., and Barber, D.L. (2001). TEL-JAK2 mediates constitutive activation of the phosphatidylinositol 3′-kinase/protein kinase B signaling pathway. J. Biol. Chem. *276*, 32704–32713.

Oltersdorf, T., Elmore, S.W., Shoemaker, A.R., Armstrong, R.C., Augeri, D.J., Belli, B.A., Bruncko, M., Deckwerth, T.L., Dinges, J., Hajduk, P.J., et al. (2005). An inhibitor of Bcl-2 family proteins induces regression of solid tumours. Nature *435*, 677–681.

Pardanani, A. (2012). Ruxolitinib for myelofibrosis therapy: current context, pros and cons. Leukemia *26*, 1449–1451.

Pardanani, A., Hood, J., Lasho, T., Levine, R.L., Martin, M.B., Noronha, G., Finke, C., Mak, C.C., Mesa, R., Zhu, H., et al. (2007). TG101209, a small molecule JAK2-selective kinase inhibitor potently inhibits myeloproliferative disorder-associated JAK2V617F and MPLW515L/K mutations. Leukemia *21*, 1658–1668.

Roberts, K.G., Morin, R.D., Zhang, J., Hirst, M., Zhao, Y., Su, X., Chen, S.C., Payne-Turner, D., Churchman, M.L., Harvey, R.C., et al. (2012). Genetic alterations activating kinase and cytokine receptor signaling in high-risk acute lymphoblastic leukemia. Cancer Cell *22*, 153–166.

Röder, S., Steimle, C., Meinhardt, G., and Pahl, H.L. (2001). STAT3 is constitutively active in some patients with Polycythemia rubra vera. Exp. Hematol. *29*, 694–702.

Santos, F.P., and Verstovsek, S. (2011). JAK2 inhibitors: are they the solution? Clin. Lymphoma Myeloma Leuk. *11* (*Suppl 1*), S28–S36.

Sayyah, J., and Sayeski, P.P. (2009). Jak2 inhibitors: rationale and role as therapeutic agents in hematologic malignancies. Curr. Oncol. Rep. *11*, 117–124.

Schwaller, J., Frantsve, J., Aster, J., Williams, I.R., Tomasson, M.H., Ross, T.S., Peeters, P., Van Rompaey, L., Van Etten, R.A., Ilaria, R., Jr., et al. (1998). Transformation of hematopoietic cell lines to growth-factor independence and induction of a fatal myelo- and lymphoproliferative disease in mice by retrovirally transduced TEL/JAK2 fusion genes. EMBO J. *17*, 5321–5333.

Silva, M., Richard, C., Benito, A., Sanz, C., Olalla, I., and Fernández-Luna, J.L. (1998). Expression of Bcl-x in erythroid precursors from patients with polycythemia vera. N. Engl. J. Med. *338*, 564–571.

Souers, A.J., Leverson, J.D., Boghaert, E.R., Ackler, S.L., Catron, N.D., Chen, J., Dayton, B.D., Ding, H., Enschede, S.H., Fairbrother, W.J., et al. (2013). ABT-199, a potent and selective BCL-2 inhibitor, achieves antitumor activity while sparing platelets. Nat. Med. *19*, 202–208.

Stein, B.L., Crispino, J.D., and Moliterno, A.R. (2011). Janus kinase inhibitors: an update on the progress and promise of targeted therapy in the myeloproliferative neoplasms. Curr. Opin. Oncol. *23*, 609–616.

Van Roosbroeck, K., Cox, L., Tousseyn, T., Lahortiga, I., Gielen, O., Cauwelier, B., De Paepe, P., Verhoef, G., Marynen, P., Vandenberghe, P., et al. (2011). JAK2 rearrangements, including the novel SEC31A-JAK2 fusion, are recurrent in classical Hodgkin lymphoma. Blood *117*, 4056–4064.

Weigert, O., Lane, A.A., Bird, L., Kopp, N., Chapuy, B., van Bodegom, D., Toms, A.V., Marubayashi, S., Christie, A.L., McKeown, M., et al. (2012). Genetic resistance to JAK2 enzymatic inhibitors is overcome by HSP90 inhibition. J. Exp. Med. *209*, 259–273.

Whitecross, K.F., Alsop, A.E., Cluse, L.A., Wiegmans, A., Banks, K.M., Coomans, C., Peart, M.J., Newbold, A., Lindemann, R.K., and Johnstone, R.W. (2009). Defining the target specificity of ABT-737 and synergistic antitumor activities in combination with histone deacetylase inhibitors. Blood *113*, 1982–1991.

Will, B., Siddiqi, T., Jordà, M.A., Shimamura, T., Luptakova, K., Staber, P.B., Costa, D.B., Steidl, U., Tenen, D.G., and Kobayashi, S. (2010). Apoptosis induced by JAK2 inhibition is mediated by Bim and enhanced by the BH3 mimetic ABT-737 in JAK2 mutant human erythroid cells. Blood *115*, 2901–2909.

Zeuner, A., Pedini, F., Francescangeli, F., Signore, M., Girelli, G., Tafuri, A., and De Maria, R. (2009). Activity of the BH3 mimetic ABT-737 on polycythemia vera erythroid precursor cells. Blood *113*, 1522–1525.